Hindawi
Wireless Communications and Mobile Computing
Volume 2022, Article ID 3709526, 17 pages
https://doi.org/10.1155/2022/3709526

Research Article

The AI-Based Channel Prediction Scheme for the 5G Wireless System in High-Speed V2I Scenarios

Zhengyu Zhang,[1] Lei Xiong,[2] Dongpin Yao,[1] and Yuanjie Wang[3]

[1]*School of Electronic and Information Engineering, Beijing Jiaotong University, Beijing, China*
[2]*Frontiers Science Center for Smart High-Speed Railway System, Beijing Jiaotong University, Beijing, China*
[3]*National Computer Network Emergency Response Technical Team/Coordination Center of China (CNCERT/CC), Beijing, China*

Correspondence should be addressed to Lei Xiong; lxiong@bjtu.edu.cn

Received 7 October 2021; Revised 18 April 2022; Accepted 23 April 2022; Published 23 May 2022

Academic Editor: Enrico M. Vitucci

Now, the fifth-generation (5G) system plays a more and more important role in the high-speed vehicle-to-infrastructure (V2I) scenario. In order to realize the high-reliability and high-efficiency transmission, it is essential to obtain accurate channel state information (CSI) for the 5G system. However, due to the fast time-varying and nonstationary characteristics of the channel in high-speed V2I scenarios, channel estimation is a challenging issue. In this paper, an artificial intelligence- (AI-) based channel prediction scheme, called AI-ChannelNet, is proposed to improve the CSI prediction performance in high-speed V2I scenarios. Specifically, AI-ChannelNet is trained in real time based on the historical channel estimation on the reference signal (RS) to realize accurate channel prediction and then recovers the received signal according to the predicted channel information. The integration of the convolutional neural network (CNN) and long short-term memory (LSTM) is designed to extract temporal features of the channel. And an online RS-based training algorithm is proposed, enabling AI-ChannelNet to track the channel variation. Evaluated by experiments, the proposed scheme outperforms conventional methods a lot, and more improvement could be achieved at a higher speed. Besides, the proposed scheme performs well without modification of the 5G radio frame and loss of transmission efficiency.

1. Introduction

In recent years, vehicle-to-everything (V2X) communication has attracted great attention in industrial and academic fields [1]. In the 3GPP specification, V2X applications include the following four types: vehicle-to-vehicle (V2V), vehicle-to-infrastructure (V2I), vehicle-to-network (V2N), and vehicle-to-pedestrian (V2P) [2]. In order to realize vehicle safety applications, dedicated short-range communication (DSRC) is developed to support V2X communication between onboard equipment (OBU) equipped on the vehicle and roadside equipment (RSU) placed on the road through short-range communication. However, DSRC technology limits the quality of service (QoS) requirements such as low data rate and short coverage [3].

Cellular V2X has the ability to overcome the short-range transmission in DSRC and realize more reliable communication. Considering the technical deployment as well as practical value, the 5G Automotive Association (5GAA) group discussed the services and developed the evolution of C-V2X standardization from the LTE-V2X to the 5G-V2X. Through the interconnection of infrastructure, vehicles, and passengers, 5G-V2X communication technologies are expected to meet not only the communication requirement of passengers but also vehicle control, safety, and information service [4], which require the wireless communication system to be able to support a massive number of sensors, low latency, ultrareliability, Gb/s transmission rate at high speed, etc. [5]. Besides, the 5G wireless communication technologies have been widely adapted to high-speed scenarios with the development of the millimeter wave [6], massive MIMO [7], nonorthogonal multiple access [8], and so on.

In order to realize the high-reliability and high-efficiency transmission, it is important to make channel

estimation, which has been proposed in the literature, i.e., least squares (LS) and minimum mean squared error (MMSE) based on specific signal structures, such as reference signal (RS), primary synchronization signal (PSS), and cyclic prefix (CP) [9–11]. Through channel estimation, channel information on the position of RS was obtained. However, the channel in high-speed V2I scenarios does not satisfy the Wide-Sense Stationary Uncorrelated Scattering (WSSUS) assumption due to high mobility; thus, the great changes in the channel state have taken place in the interval of RS [12]. Thus, it is essential to obtain accurate channel state information on payload symbols, i.e., non-RS via channel prediction.

Generally speaking, the channel prediction was realized by interpolation methods, including the nearest interpolation, linear interpolation, Gaussian interpolation, and Sinc interpolation [13, 14]. Compared with other wireless communication technologies, there are nonnegligible challenges in channel prediction due to the higher frequency band and up to 500 km/h mobility in the 5G communication system, resulting in the higher Doppler shift and the shorter coherence time. The conventional prediction methods no longer perform well due to the fast time-varying and nonstationary characteristics. However, the prediction performance can be improved by additional RS [15], which not only reduces the transmission efficiency but also requires the modification of radio frames. However, an artificial intelligence- (AI-) based channel scheme has the ability to extract time-domain features and learn temporal channel regularity, in which the historical wireless data and scenario data on the same track can aid the channel prediction for high-speed scenarios and can be applied in the 5G system to enhance the accuracy and improve the limitation of conventional methods [16].

Rapidly developing AI technology provides innovative solutions for the challenges of the communication system, such as channel estimation and detection [17], channel decoding [18], and channel recognition [19]. Specifically, the prediction on the fast time-varying and nonstationary channel based on AI has attracted a lot of attention [20]. [21] proposed a channel state information (CSI) prediction scheme, which achieves similar performance to traditional methods through the joint learning framework of the convolutional neural network (CNN) and long short-term memory (LSTM) but costs less computing time. [22] developed a prediction scheme of multipath link quality in the millimeter-wave system based on LSTM and verified the great prediction performance. [23] presented an adaptive channel prediction scheme based on RNN, which predicts the nonstationary and time-varying channel by learning historical data. However, in order to make the prediction about the fast time-varying and nonstationary channel, most of the proposed algorithms were developed based on the data-driven neural network, in which the prediction accuracy depends on a large number of known training data. Once there is a deviation between the actual channel and the training dataset, the prediction performance will greatly degrade [24], while the model-driven neural network is more suitable for channel prediction in high-speed scenarios due to the low demand for datasets, low risk of overfitting, and flexible application deployment [25].

In this paper, we propose a novel AI-based channel prediction scheme, called AI-ChannelNet, for the 5G wireless system in high-speed V2I scenarios. The AI-ChannelNet is trained in real time based on the historical channel estimation on RS to realize accurate channel prediction and then recovers the received signal according to predicted channel information. The optimized model is experimented over the WINNER D2a channel model to validate the performance in high-speed scenarios. The main contributions of this paper are as follows:

(1) An AI-based channel prediction scheme for 5G wireless communications in high-speed V2I scenarios was proposed to reconstruct the CSI

(2) A learning framework based on CNN was developed to extract the temporal regularity to make channel prediction

(3) An online RS-based training strategy was developed to adjust the CNN predictor dynamically and track the time-varying and nonstationary channel

(4) A hybrid deep-layer network was developed to map the relationship between the channel information and the received signal to recover transmitted data

The remainder of the paper is organized as follows. We first briefly introduce the channel characteristics, the system model, and the reference signal in the 5G system in Section 2. Then, we describe the proposed channel prediction scheme in detail, including the workflow, the architecture and dataflow, and the training in Section 3. Afterward, the experiment results and analysis are provided in Section 4. Finally, the conclusions are drawn in Section 5.

2. Channel Prediction in High-Speed V2I Scenarios

2.1. Channel Characteristics. Due to the terrain and electromagnetic characteristics, the special high-speed V2I scenarios, such as expressway and high-speed railway (HSR), have a significant impact on radio propagation. For the diverse high-speed V2I scenarios, the characteristics of the channel, such as Doppler shift, multipath delay, and angle spread, change rapidly and significantly with time; i.e., the channel appears to be fast time-varying and nonstationary.

Figure 1 shows a typical high-speed V2I scenario. Due to the open space and the antennas of gNB being usually 20-30 m higher than roads, the line of sight (LOS) is the dominant propagation mechanism. In practice, the channel performs special characteristics in high-speed V2I scenarios. In [26], the region can be divided into two areas for modeling. (1) UE is in the vicinity of gNB, where the LOS path is affected by the angle of the antenna pattern. (2) UE is far away from gNB, where the LOS path is affected by the propagation distance. The regularity of the channel, which

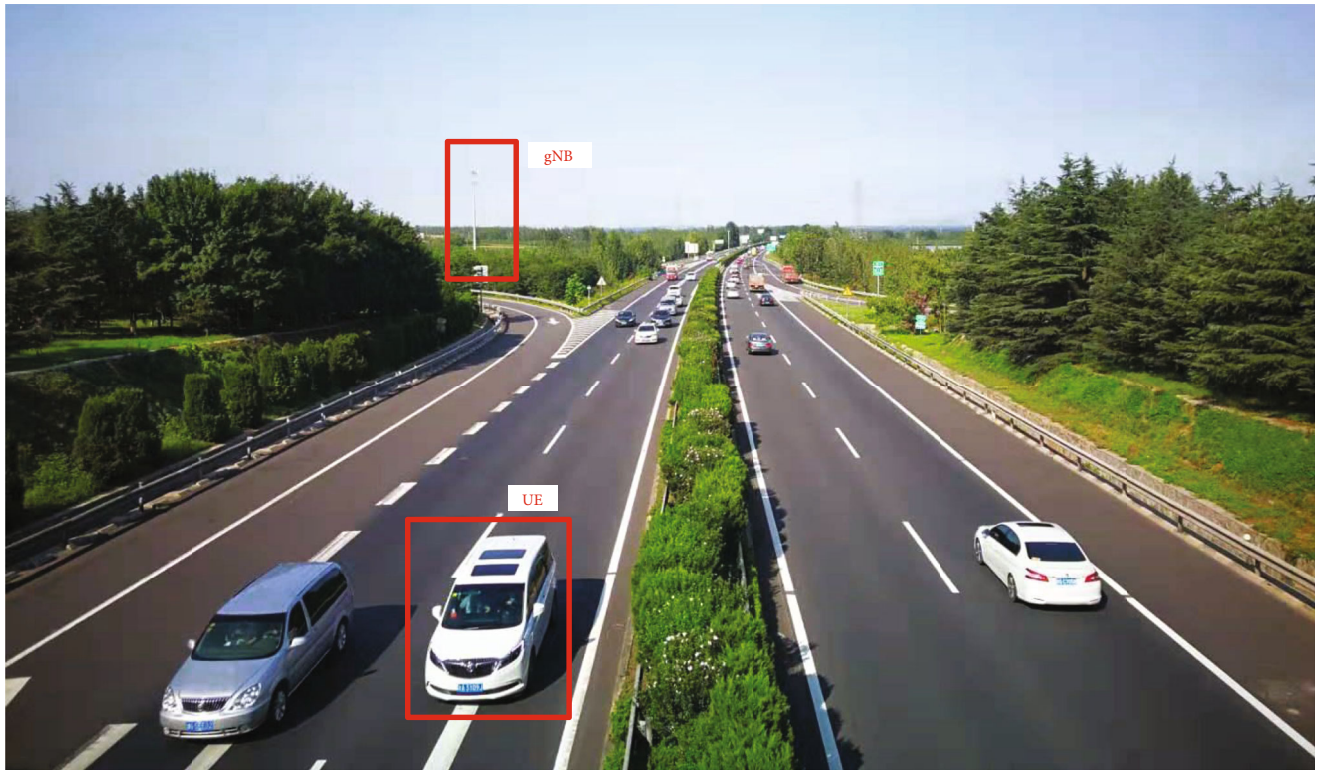

Figure 1: The typical high-speed V2I scenario.

describes instantaneous state variation, is significantly different between these two regions.

Furthermore, the dynamic variation patterns of channel characteristics, such as path loss (PL), Ricean K factor, Doppler frequency shift, and channel impulse response (CIR), were studied through the measurements in [27]. For instance, the Doppler shift of LOS sweeps a lot as the UE passes through the gNB and maintains the maximum value when UE is far away from gNB with stable speed, as shown in Figure 2.

As aforementioned, lots of measurements have illustrated that although the channel performs obvious fast time-varying and nonstationary characteristics in high-speed V2I scenarios, the channel characteristics have obvious variation patterns and predictable characteristics due to the linear arrangement of gNB along the track, the relatively stable speed of UE, etc., which are expected to provide more accurate channel prediction via AI technology and improve the communication performance.

2.2. The System Model. For the high-speed V2I scenarios, consider a 5G wireless system with N subcarriers, N_r receiver antennas, and N_t transmitter antennas. Let $X(t) = [x(t)^1, \cdots, x(t)^{N_t}]^T$ be the transmitted signal, with $x(t)^i = [x(t)_0^i, \cdots, x(t)_{N-1}^i]^T$ being the signal vector transmitted from the i-th antenna, $i = 1, \cdots, N_t$. We denote the received signal by $Y(t) = [y(t)^1, \cdots, y(t)^{N_r}]^T$, where $y(t)^j$ is the received OFDM symbol on the j-th receiver antenna, $j = 1, \cdots, N_r$. The received signal is shown below:

$$Y(t) = H(t)X(t) + N(t), \tag{1}$$

where $N(t)$ represents the complex Gaussian noise vector at time t. Furthermore, the complex channel matrix $H(t)$ of size (N_r, N_t) is given by the following:

$$H(t) = \begin{bmatrix} h_{11}(t) & \cdots & h_{1N_t}(t) \\ \vdots & \ddots & \vdots \\ h_{N_r1}(t) & \cdots & h_{N_rN_t}(t) \end{bmatrix}, \tag{2}$$

where $h_{ji}(t)$ represents the complex channel coefficient of the subchannel from the i-th transmitter antenna to the j-th receiver antenna.

The RS that is already known to both the transmitter and the receiver is transmitted for channel estimation. The estimated channel coefficient $\widehat{h}_{ji}(m)$ on the m-th RS can be derived from the received RS as follows:

$$\widehat{h}_{ji}(m) = \frac{y(m)^j}{p(m)^i} = h_{ji}(m) + \tilde{h}_{ji}(m), \tag{3}$$

where $y(m)^j$, $p(m)^i$, and $\tilde{h}_{ji}(m)$ represent the received signal on the j-th receiver antenna, the known RS from the i-th transmitter antenna, and channel estimation errors, respectively, on the m-th RS position. In practice, the estimated

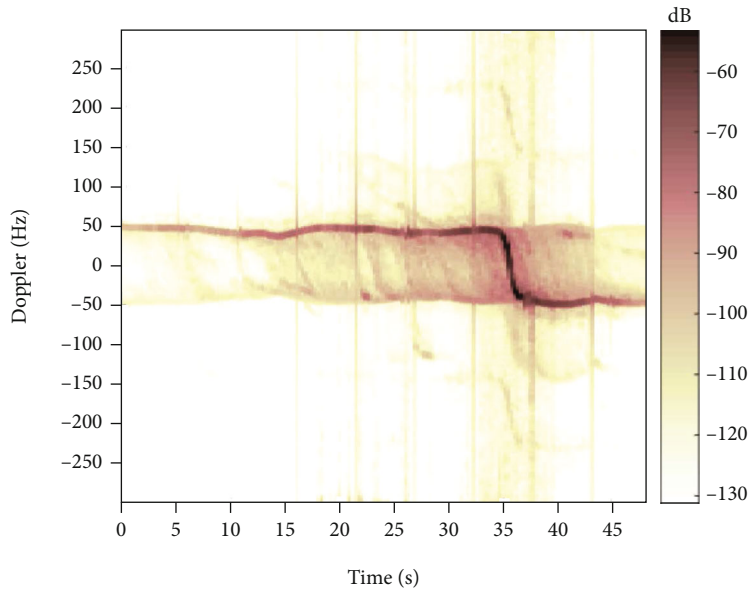

Figure 2: The measured dynamic Doppler shift in V2I scenarios [26].

channel coefficient $\widehat{h}_{ji}(m)$ is discrete due to the discrete RS. To obtain accurate channel information, interpolation methods are employed to predict the channel on payload symbols.

2.3. Reference Signal in the 5G System. The prediction performance of conventional methods is affected by the allocation of RS, which is related to the radio frame structure. Different from other communication systems, the number, position, and density of RS in the 5G system are configurable, as shown in Figure 3. For the radio frame (normal CP) of 5G, there are ten subframes in each radio frame, two slots in each subframe, and fourteen OFDM symbols in each slot, which contains one RS and thirteen payload symbols, respectively. The RS distributes discretely in the time and frequency domains; thus, the accurate channel information needs to be predicted by interpolation.

The higher frequency band of 5G and higher speed in high-speed V2I scenarios result in the higher Doppler shift and the shorter coherence time. The coherence time can be calculated as follows:

$$T_{\text{coh}} \approx \frac{1}{2\pi f_{\text{d,max}}}, \tag{4}$$

where $f_{\text{d,max}}$ is the maximum Doppler shift.

For the 5.9 GHz frequency band, which has become the premier option for commercial V2I scenario deployments [28], the coherence time T_{coh} is 0.24 ms when $v = 120$ km/h . In this case, the coherence time is shorter than the duration of one slot and the channel in the interval of RS changes significantly.

For the 5G wireless system in high-speed V2I scenarios, an additional RS is added to the slot, named 5G-addition in the 3GPP TS 38.211 [29], as shown in Figure 3. More RS help track the channel in high-speed V2I scenarios with the loss of the transmission efficiency slightly.

3. AI-ChannelNet

The AI-ChannelNet was introduced in this section from three aspects: the workflow, the architecture and dataflow, and the training methods.

3.1. Workflow. For the time domain, the channel between adjacent RS performs temporal regularity due to the fast time-varying channel and the linear gNB arrangement in high-speed V2I scenarios. For the frequency domain, the channel between adjacent subcarriers changes moderately. Therefore, the AI scheme was developed to make the time-domain prediction and the linear interpolation method was used in the frequency-domain prediction. The workflow of AI-ChannelNet is shown in Figure 4 with four steps as follows:

(1) The AI-ChannelNet predicts the channel information on the non-RS position based on the learned channel regularity in the time domain

(2) The linear interpolation is employed to predict the channel information on the non-RS position in the frequency domain. Note that the learned channel regularity of AI could not be generalized along the subcarriers and the negative impact caused by high mobility is mainly reflected in the time domain

(3) The predicted channel information and received signal are redefined as the CSI image and signal image, respectively, which have the real-part channel and imaginary-part channel. For these images, each pixel represents an OFDM symbol and corresponding channel information. The length and width of the

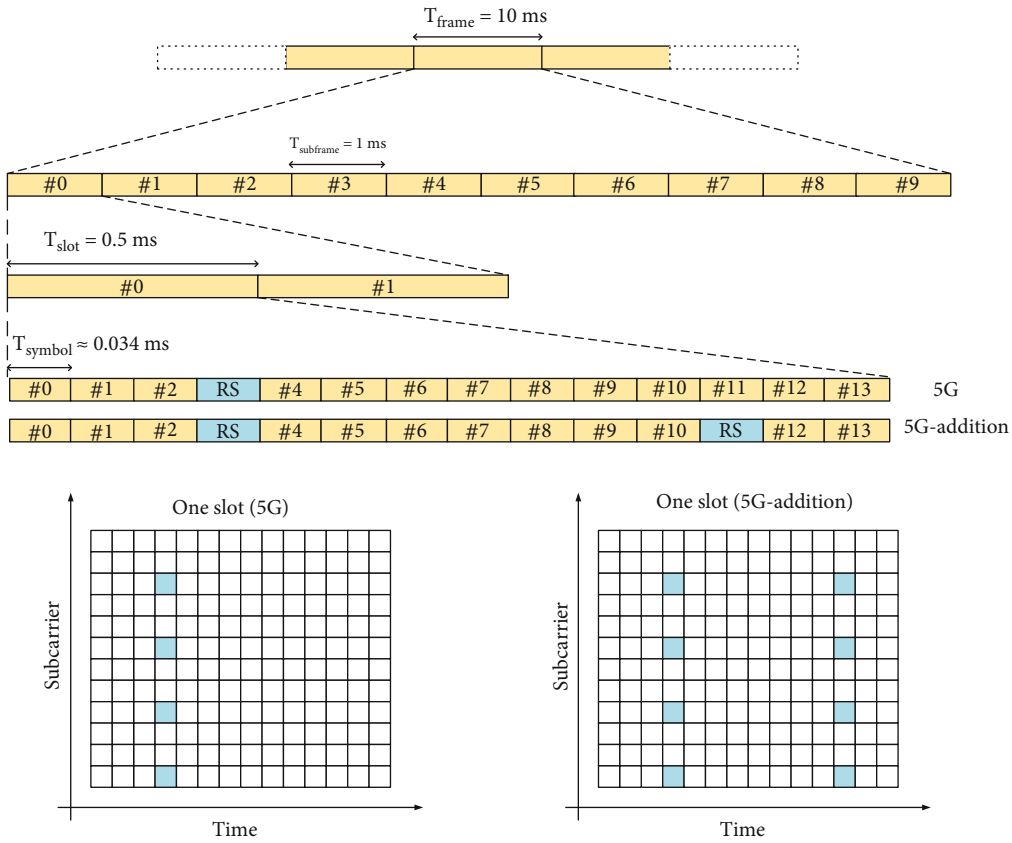

Figure 3: The allocation of RS in the 5G system (the spacing of the subcarriers is 30 kHz).

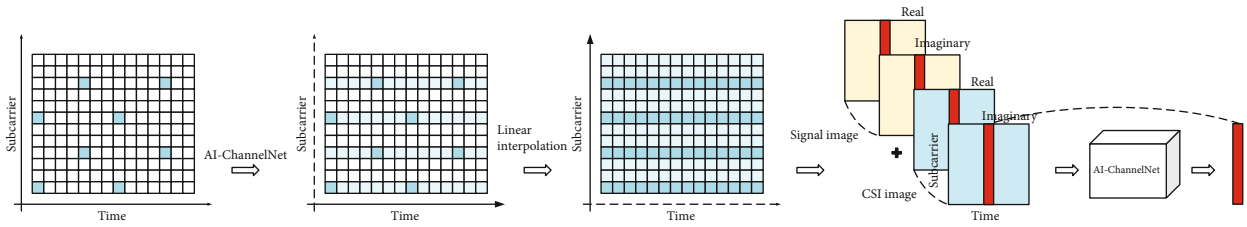

Figure 4: The workflow of AI-ChannelNet.

image represent time and different subcarriers, respectively

(4) Through feeding the CSI image and signal image simultaneously, the AI-ChannelNet outputs the recovered transmitted signal

3.2. Architecture and Dataflow. Figure 5 shows the architecture of AI-ChannelNet, which contains the CNN and LSTM to predict channel information and recover received signals, respectively. The convolution layer, pooling layer, and fully connected layer are designed in CNN to simplify the architecture and adapt to the online training algorithm with the complexity as low as possible. The LSTM layer and convolution layer are designed in LSTM to learn the relationship between the received signal, the channel information, and the transmitted signal with the complexity as sufficient as possible.

In AI-ChannelNet, the dataflow is divided into two lines: the dataflow of RS and the dataflow of the received signal (including payload symbols).

3.2.1. The Dataflow of RS. For the dataflow of RS, the latest RS is used to determine whether the weights of AI-Channel Net need to be updated. Then, it is stored in the historical buffer for a period of time, which is employed as the dataset for the online training algorithm. Before being fed into AI-ChannelNet, the RS needs to be preprocessed via the two-dimensional process and shift. The two-dimensional process is to process the complex-valued channel information into real and imaginary parts, respectively. The shift is to split the original data into multiple continuous time series by a historical window with constant length. The input and label of training and the input and output of prediction are shown as follows, respectively:

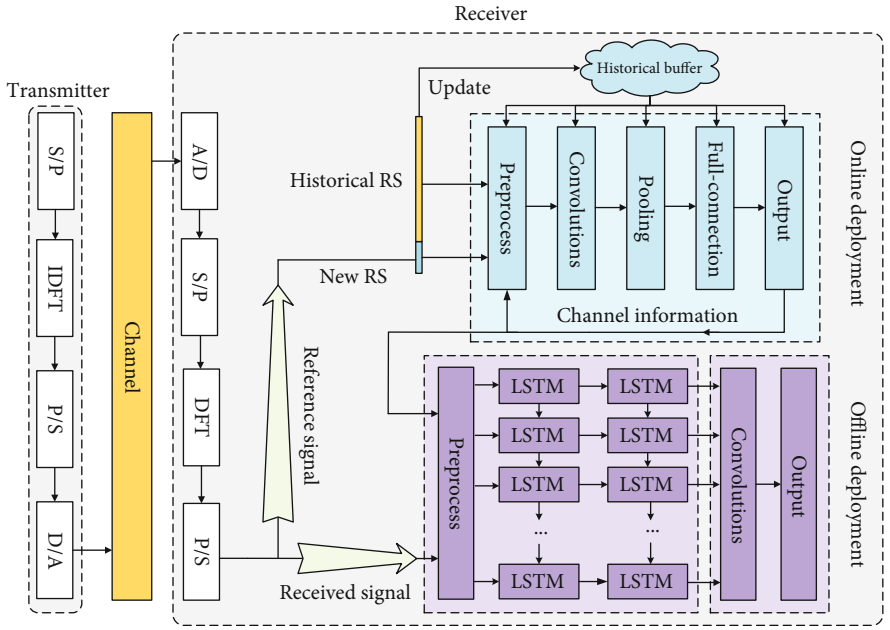

Figure 5: The architecture of AI-ChannelNet.

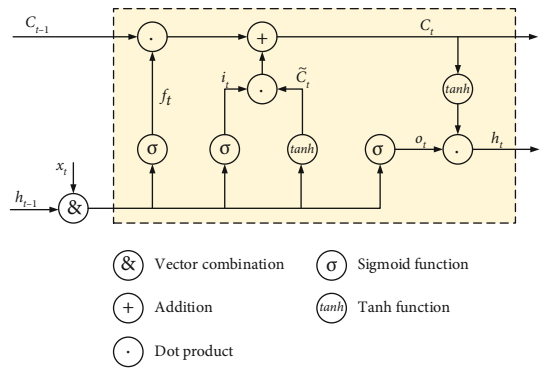

Figure 6: Architecture of the LSTM unit.

For training, we have the following:

$$\begin{cases} \text{Input} : h(m-k,0), \cdots, h(m-1,0), h(m,0), \\ \text{Label} : h(m+1,0). \end{cases} \tag{5}$$

For prediction, we have the following:

$$\begin{cases} \text{Input} : h(m-k,q), \cdots, h(m-1,q), h(m,q), \\ \text{Output} : h(m+1,q), q \in \{1,2,\cdots,N-1\}, \end{cases} \tag{6}$$

where $h(m,0)$ is the channel coefficient on the m-th RS; $h(m,q)$ is the channel coefficient on the q-th payload symbol after the m-th RS; k is the constraint length, which represents how much historical information the single prediction depends on; $q \in \{1,2,\cdots,N-1\}$ is the index of payload symbols; and N is the number of symbols in the interval of RS.

After preprocessing, convolution operation occurs in the time dimension to extract the temporal features from the real component and imaginary component, which is equivalent to carrying out the one-dimensional convolution operation on two-dimensional data. The extracted features are reflected in the feature map, which is calculated as follows:

$$Z^p = W^p \otimes X + B^p = \sum_{d=1}^{2} W^{p,d} \otimes X^d + B^p, \tag{7}$$

where Z^p is the p-th feature map, which is extracted by the p-th convolution kernel W^p, and $X = [h_1, h_2, \cdots, h_k]$ is the input vector. B^p is the bias of the p-th convolution kernel, d is the dimension of vectors, and $\otimes$ is the convolution operation. With the convolution kernel size m, the calculation process of z_i in the feature map Z^p is shown as follows, where w, b, and h are the elements of W^p, B^p, and X:

$$z_i = \sum_{u=1}^{m} \sum_{d=1}^{2} w_{u,d} \cdot h_{i+u-1,d} + b_i. \tag{8}$$

For the time series prediction problem based on the neural network, the mean squared error (MSE) is often used to train the loss function of the process. But in channel prediction, the object of prediction is the complex coefficient, so this paper considers the Error Vector Magnitude (EVM) as the loss function of the training process to measure the similarity between the target value and the output value so as to improve the learning effect. The EVM loss function is calculated as follows:

$$L_{\text{evm}} = \sqrt{\frac{\sum_{n=1}^{N} \left| \widehat{h}_n - h_n \right|^2}{\sum_{n=1}^{N} |h_n|^2}}, \tag{9}$$

Input: The historical buffer length l
The update threshold α
The loss threshold β
Initialize: The number of epochs n
The update sensitivity r
The update counter $c = 0$
The historical buffer $\Theta = [h(m-l,0), h(m-l+1,0), \cdots, h(m,0)]$
The weights of CNN which are trained by the buffer
Output: The predicted values on payload symbols
while the value on the latest RS position h_e is estimated **do**
The value on the latest RS position h_p is predicted by CNN based on the Θ.
Update the Θ by
for $i = 0 : l - 1$ **do**
$h(m-1-i,0) \longleftarrow h(m-i,0)$
end for
$h(m,0) \longleftarrow h_e$
$l_{\text{evm}} \longleftarrow \text{Evm}(h_e, h_p)$
if $l_{\text{evm}} > \alpha$ **then**
$c \longleftarrow c + 1$
if $c > r$ **then**
$c \longleftarrow 0$
CNN is trained based on the Θ:
$p = 0$
if $p < n$ **then**
$l_{\text{evm}} \longleftarrow \text{Adam}(L_{\text{evm}}, \Theta)$
if $l_{\text{evm}} > \beta$ **then**
Break
else
$p \longleftarrow p + 1$
end if
end if
end if
end if
Predict the values on payload symbols
end while

Algorithm 1: Online RS-based training for AI-ChannelNet.

Table 1: The difference of online and offline neural network deployment.

	Online deployment	Offline deployment
Learning object	Temporal channel regularity	Mapping from the received signal to the transmitted signal
Input information	Channel value on the RS position	Mapping from the received signal to the transmitted signal
Output information	Channel prediction on the payload symbol position	Estimated transmitted signal
Function	Track channel	Signal recovery
Network baseline	CNN	LSTM+CNN
Training method	Online RS-based training method	Offline classification training method

where h_n and $\widehat{h}_n$, $n = 1, \cdots, N$, are the label values and predicted values, and N is the number of training samples.

3.2.2. The Dataflow of the Received Signal. For the dataflow of the received signal, they are fed into AI-ChannelNet together with predicted channel information. The temporal relationship between the received signal and the channel information is extracted by LSTM, and then the recovery process is treated as the classification problem to output the transmitted signal. The architecture of the LSTM unit is shown in Figure 6. LSTM neural network transmits cyclic information by introducing the internal state C_t and output data features to the external state s_t, calculated as follows:

$$C_t = f_t \odot C_{t-1} + i_t \odot \tilde{C}_t, \tag{10}$$

Table 2: The channel and scenario parameters.

Parameters	Value
Channel model	WINNER D2a
Number of links	100
Segment distance	10 m
Coverage radius of gNB	500 m
Vertical distance between the gNB and the track	50 m
Moving speed	90-150 km/h

$$s_t = o_t \odot \tanh\,(C_t), \tag{11}$$

where $\tilde{C}_t$ is the candidate status, and f_t, i_t, and o_t are the forget gate, the input gate, and the output gate, respectively, defined as follows:

$$\tilde{c}_t = \tanh\,(W_c[s_{t-1}, x_t] + b_c), \tag{12}$$

$$f_t = \sigma\big(W_f[s_{t-1}, x_t] + b_f\big), \tag{13}$$

$$i_t = \sigma(W_i[s_{t-1}, x_t] + b_i), \tag{14}$$

$$o_t = \sigma(W_o[s_{t-1}, x_t] + b_o), \tag{15}$$

where $W_{c,f,i,o}$ and $b_{c,f,i,o}$ are weight matrices and bias vectors, x_t is the current input, s_{t-1} is the hidden state at the previous moment. The standard sigmoid function $\sigma(\cdot)$ and the hyperbolic function $\tanh(\cdot)$ are defined as follows:

$$\sigma(x) = \frac{1}{1 + e^{-x}}, \tag{16}$$

$$\tanh\,(x) = \frac{e^{x} - e^{-x}}{e^{x} + e^{-x}}. \tag{17}$$

For the three gates, the forget gate f_t, the input gate i_t, and the output gate o_t control the information that needs to be forgotten in the C_{t-1}, the information that needs to be saved in the $\tilde{C}_t$, and the data that needs to be output to the h_t, respectively.

Then, the temporal relationship extracted by LSTM is fed into the convolution layer to the recovery signal. The category label is $\{1, 2, 3, \cdots, 2^M\}$, where M is the modulation order. The output layer is designed as the softmax layer, where the number of nodes K is equal to the number of categories. Assume that the output value of the i-th node is p_i. Then, the probability that belongs to i in the output layer is as follows:

$$P_i = \frac{e^{p_i}}{\sum_{j=1}^{K} e^{p_j}}. \tag{18}$$

Correspondingly, the loss function of training is the cross-entropy function as follows:

$$L_{\text{cross-entropy}} = -\frac{1}{N}\sum_{n=1}^{N}\sum_{i=1}^{K} I_{i,n} \log\,(P_{i,n}), \tag{19}$$

where $I_{i,n}$ is the indicator vector (1 represents the n-th sample that belongs to the category i, and 0 represents not), and N is the number of training samples.

3.3. Training. The training of AI-ChannelNet includes two strategies: online RS-based training and offline classification training, which are aimed at tracking the dynamic channel in real time and learning the certain mapping, respectively.

3.3.1. Online RS-Based Training. AI-ChannelNet is trained via the online RS-based training algorithm to track the dynamic channel and realize the accurate channel prediction. The online RS-based training algorithm is shown as Algorithm 1.

The historical buffer length l represents the memory capacity of the buffer: too large will increase the convergence time of each iteration, and too small will result in poor tracking performance.

The update threshold α is introduced as the trigger of the online training algorithm, which is used to determine whether the network is updated or not.

The update sensitivity r is set to reduce the update frequency, avoiding successive updates when the channel changes suddenly.

The early-stop strategy based on the loss function is adapted in online training to speed up the convergence, in which the optimizer is terminated once the loss function value exceeds threshold β.

3.3.2. Offline Classification Training. For the offline training, the massive volume of historical data, including the channel information, received signal, and transmitted signal, is conducted as the training samples to learn the mapping from the received signal to the transmitted signal. Then, the loss function is reduced by using the Adam optimizer based on the backpropagation. As a result, we obtain a well-trained neural network which can be implemented offline.

The proposed scheme includes online deployment and offline deployment with differences in terms of the learning object, input and output information, function, network baseline, and training method, which are compared in Table 1.

4. Numerical Results

Compared with the conventional methods, the prediction performance and reliability of AI-ChannelNet are evaluated in this section. Furthermore, the simulation data generated by the WINNER D2a channel is tested in the experiment.

4.1. Channel Characteristics of the WINNER D2a Model. At present, there are fewer standard channel models for V2I scenarios, especially under high speed; thus, the approximate WINNER channel model was used in the experiment in this section.

The WINNER II channel model is a link-level and system-level simulation model for broadband communication systems such as LTE and 5G systems. Propagation scenario D2a represents radio propagation in environments where the UE are moving at a very high speed in a rural area

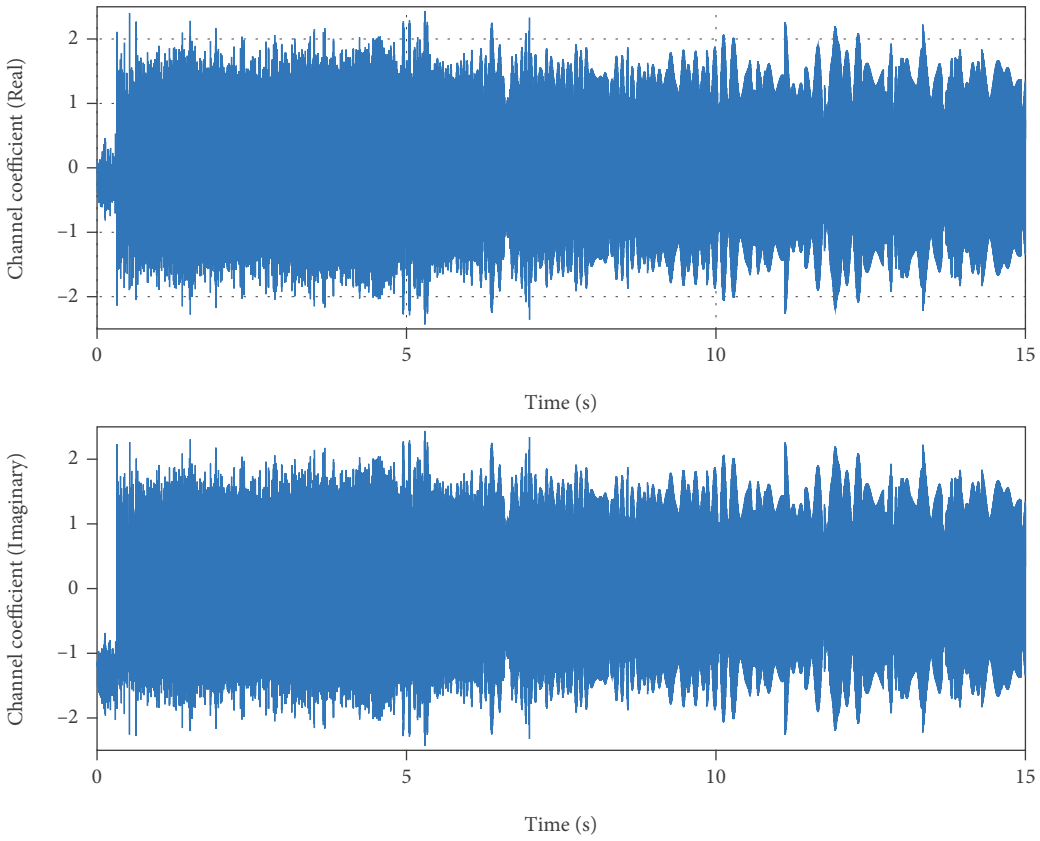

Figure 7: The fast time-varying characteristic of the WINNER D2a channel.

[30]. In this condition, the WINNER D2a model is a widely used standard channel model for high-speed moving scenarios and is suitable for high-speed V2I scenarios. The simulation parameters are shown in Table 2.

Figure 7 shows the channel variation over the whole coverage of gNB when $v = 120$ km/h. It can be seen that the channel coefficient changes rapidly in the time domain and the WINNER D2a channel performs an obvious fast time-varying characteristic.

Figure 8(a) shows the Doppler shift variation with distance from the gNB, which accord well with the measurement results mentioned in Section 2.1. Figure 8(b) shows the channel coefficient in the typical positions, which are in the vicinity of gNB and far away from the gNB, respectively. It can be seen that the channel coefficient changes with predictable characteristics in the time domain when UE is far away from gNB and the WINNER D2a channel performs an obvious nonstationary characteristic.

4.2. Prediction Performance. To validate the performance of the proposed scheme, the parameters of AI-ChannelNet are optimized firstly through lots of experience experiments and are presented in Table 3.

Figure 9 shows the real part of channel prediction results along the time when $v = 120$ km/h, which is similar to the imaginary part. From this figure, we can find that the prediction results are very close to the ground truth. With the UE far away from the gNB, the regularity of the channel tends to be obvious and the prediction performance becomes better. This result implies that the AI-ChannelNet is beneficial to channel prediction in high-speed V2I scenarios.

Figure 10 shows the prediction performance of AI-ChannelNet and conventional methods in the whole gNB coverage when $v = 120$ km/h. For the 5G radio frame, it is not able to meet the requirement of communication through conventional methods with an unacceptable EVM of 36% and more, while that of AI-ChannelNet is 15% to 3%. In order to improve the prediction performance of conventional methods, the 5G-addition radio frame is employed to conduct experiments. Although the EVM of the nearest, linear, Gaussian, and Sinc methods decreases to 26%, 14%, 11%, and 8%, respectively, it is still higher than that of the AI-ChannelNet. Besides, the AI-ChannelNet performs better when the UE is far away from the gNB as the regularity of the channel becomes more obvious.

Figure 11 shows the comparison of AI-ChannelNet and conventional methods on the 5G-addition radio frame when $v = 120$ km/h. It can be seen that the prediction result of AI-ChannelNet is more close to the perfect channel. The second is the Sinc method with some distortion points. The prediction results of the Gaussian, linear, and nearest methods are seriously distorted.

Tables 4 and 5 show that the prediction performance varies with speed on the 5G and 5G-addition radio frames, respectively. It can be seen that AI-ChannelNet performs better than conventional methods in high-speed moving

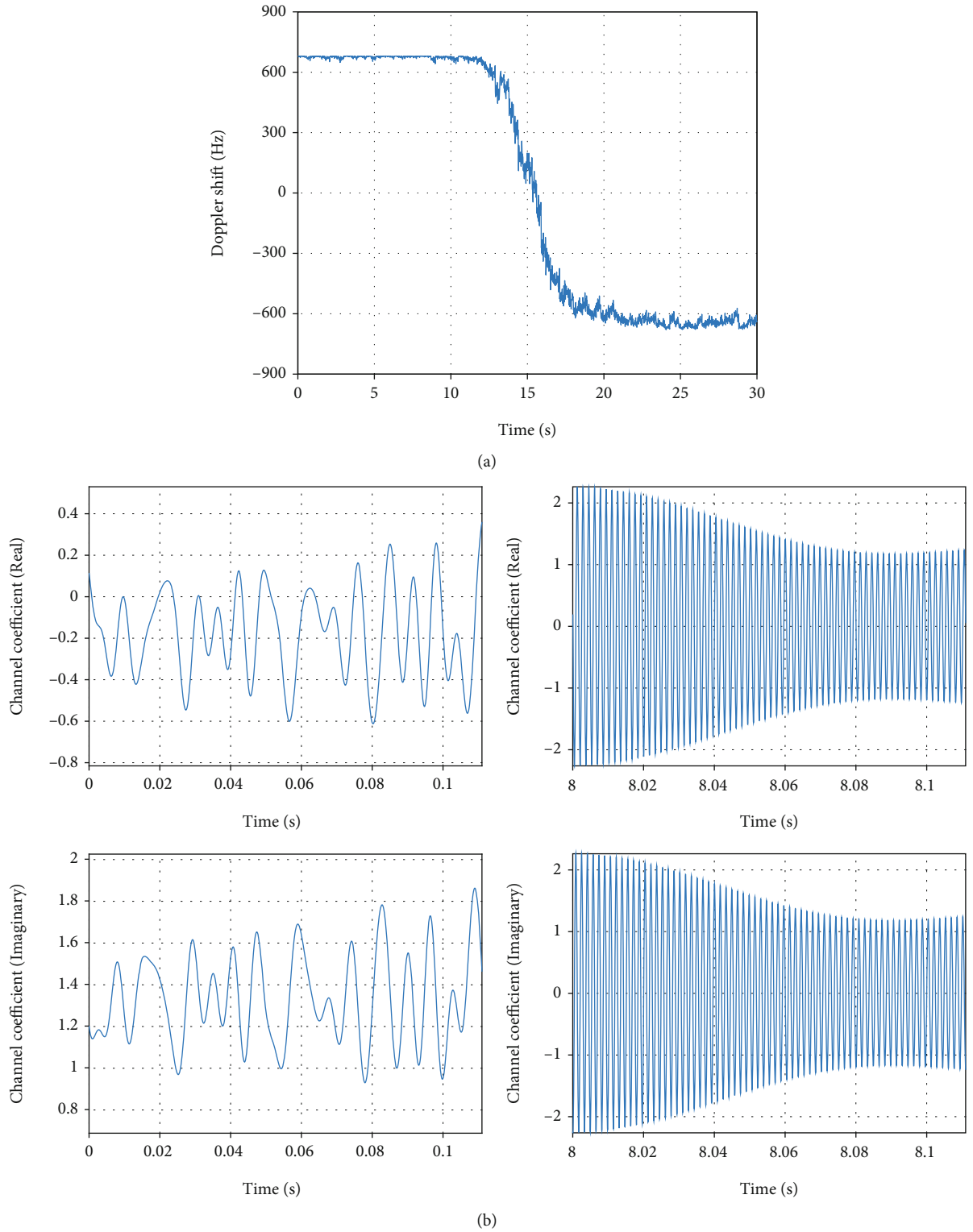

Figure 8: The nonstationary characteristic of the WINNER D2a channel. (a) Doppler shift variation with distance from the gNB. (b) The channel coefficient when UE is in the vicinity of gNB (left) and UE is far away from gNB (right).

Table 3: The AI-ChannelNet parameters.

Parameters	Value
Number of convolution kernels	8
Size of convolution kernels	1×3
Number of units in the fully connected layer	128
Number of LSTM units	64
Constraint length	80
Historical buffer length	15
The update threshold	0.015
The loss threshold	0.015
The update sensitivity	2
Epochs	300
Batch size	50
Optimization	Adam
Loss function	EVM and cross-entropy
Learning rate	0.001

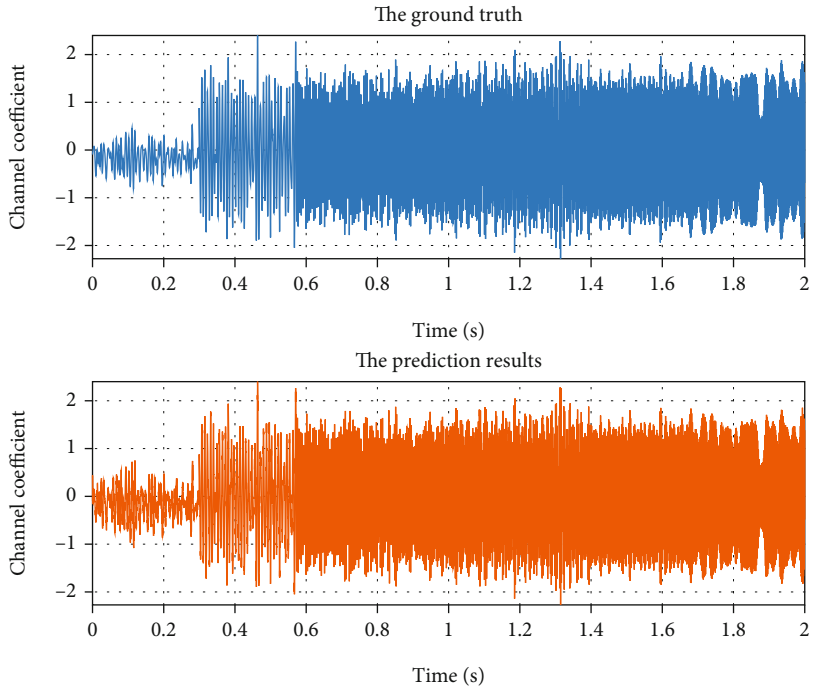

Figure 9: The real part of the ground truth and prediction results of AI-ChannelNet.

scenarios. For instance, EVM of Sinc methods on the 5G radio frame increases from 7.89% to 39.24% with 90 km/h to 140 km/h while that of AI-ChannelNet is about 4%. Note that the higher the speed is, the more improvement can be obtained by AI-ChannelNet.

4.3. Reliability. The 5G wireless communication system parameters are shown in Table 6. Figure 12 shows the CSI image predicted by AI-ChannelNet when $v = 120$ km/h, which is used to recover the received signal. The X-Y-Z axis corresponds to the slot (time domain), the subcarrier (frequency domain), and the CSI image pixels (channel information), respectively. It can be seen that the CSI images on different radio frames are similar, which are both close to the perfect CSI images. The figure illustrates that AI-ChannelNet can achieve acceptable prediction performance on the 5G radio frame so as to reduce the number of RS and improve the transmission efficiency in high-speed V2I scenarios.

Figure 13 shows the BER of different methods on the 5G radio frame when $v = 120$ km/h. For conventional methods, the communication systems are not able to work normally due to poor prediction performance while AI-ChannelNet performs well with low BER. Although the performance of

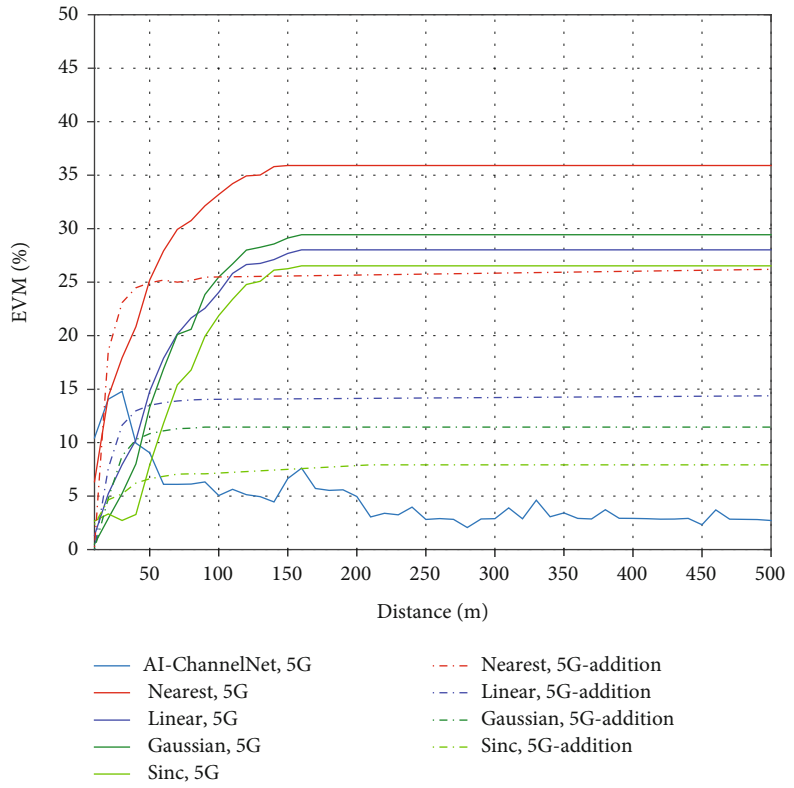

Figure 10: The prediction performance of AI-ChannelNet and conventional methods with distance from the gNB.

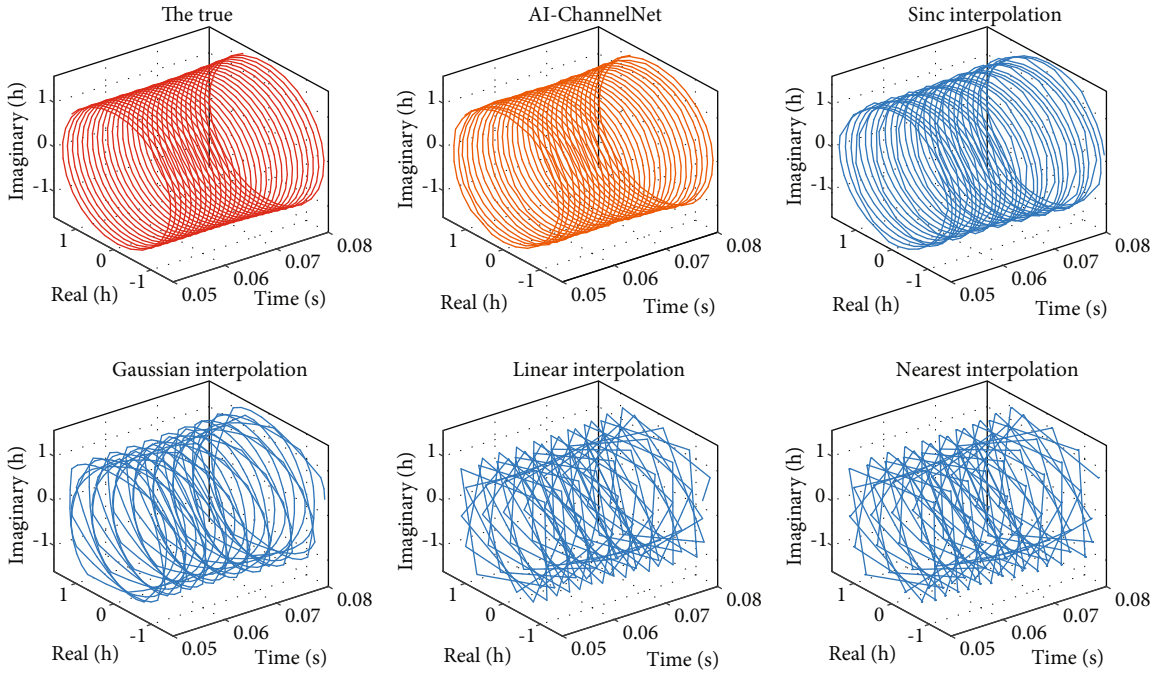

Figure 11: The comparison of AI-ChannelNet and conventional methods.

Table 4: The prediction performance varies with speed on the 5G radio frame.

EVM (%)	90 km/h	100 km/h	110 km/h	120 km/h	130 km/h	140 km/h	150 km/h
AI-ChannelNet	3.13	3.41	3.68	4.06	4.20	4.40	4.71
Nearest	19.46	23.65	27.58	35.25	37.44	39.24	43.48
Linear	9.38	15.08	22.82	28.16	38.18	42.45	45.82
Gaussian	8.62	13.86	20.98	26.01	35.09	39.02	42.12
Sinc	7.89	8.49	16.27	24.66	33.25	37.14	39.24

Table 5: The prediction performance varies with speed on the 5G-addition radio frame.

EVM (%)	90 km/h	100 km/h	110 km/h	120 km/h	130 km/h	140 km/h	150 km/h
AI-ChannelNet	3.51	3.79	3.83	4.41	4.59	5.25	5.69
Nearest	14.13	18.60	21.11	25.45	29.88	33.16	35.97
Linear	5.20	7.76	10.78	13.85	19.84	25.25	28.94
Gaussian	2.80	4.47	7.45	11.07	17.25	22.35	28.92
Sinc	7.29	7.64	7.30	7.76	10.49	14.53	21.37

Table 6: 5G wireless communication system parameters.

Parameters	Value
Carrier frequency	5.9 GHz
Bandwidth	50 MHz
Number of resource blocks	133
Cyclic prefix	Normal
Modulation	16QAM
Spacing of subcarriers	30 kHz
Channel coding scheme	LDPC
Code rate	0.5
SNR	0 to 10 dB

conventional methods can be improved by increasing the RS, it needs excessive consumption of transmission resources. Thus, the proposed AI-ChannelNet is expected to be applied to communication systems at ultrahigh speed.

Figure 14 shows the throughput of different methods on the 5G radio frame when $v = 120$ km/h. It can be seen that AI-ChannelNet performs higher throughput than conventional methods. When SNR increases, the advantage of AI-ChannelNet becomes more obvious due to the accurate channel prediction. Although the strategy that increasing RS improves channel prediction performance and decreases BER in conventional methods, resulting in better throughput, it is negative for AI-ChannelNet due to additional transmission cost. As mentioned above, AI-ChannelNet outperforms others with high throughput as well as low BER, which is expected to realize the high-reliability and high-efficiency transmission in high-speed V2I scenarios.

For comparison, the adaptive and parameter-free recurrent neural structure (APF-RNS) [23], which was used for real-time prediction in the dynamically nonstationary channel, is also simulated. It can be observed that both methods can present more accurate channel prediction results under higher SNR. However, the proposed method is more suitable for high-speed conditions, especially in higher SNR, which performs far lower BER and higher throughput than that of APF-RNS. This demonstrates the effectiveness of our proposed method in the high-speed scenario. Besides, the proposed method has the advantages that cannot be shown in the figure as follows:

(1) A smaller neural network scale than APF-RNS corresponds to a faster convergence speed

(2) Channel information is required only in the position of RS, while the successive channel data is required for training in APF-RNS

4.4. Computation Complexity. The floating point of operations (FLOP), which represents the total computational cost, has been introduced as the measurement of computation complexity in deep learning research widely [31, 32]. As a standard convolution layer, the FLOP is calculated as follows:

$$\mathrm{FLOP} = {D_k}^2 \cdot N_f \cdot N_c \cdot {D_F}^2, \tag{20}$$

where D_k is the kernel size, N_f is the number of filters, N_c is the number of channels, and D_F is the size of the feature map. For the optimized parameters of the CNN predictor, the FLOP values are shown in Table 7.

It can be seen that the computational complexity of the forward propagation is 5120 FLOP. Besides, the CNN is trained by the online real-time training algorithm; thus, the computational cost of backpropagation is indispensable. Considering that the maximum number of epochs is set as 300 and the historical buffer length is optimized as 15, the maximum FLOP, including training and prediction, is 46.08M FLOP. In fact, the average FLOP is less than it due to the early-stop strategy.

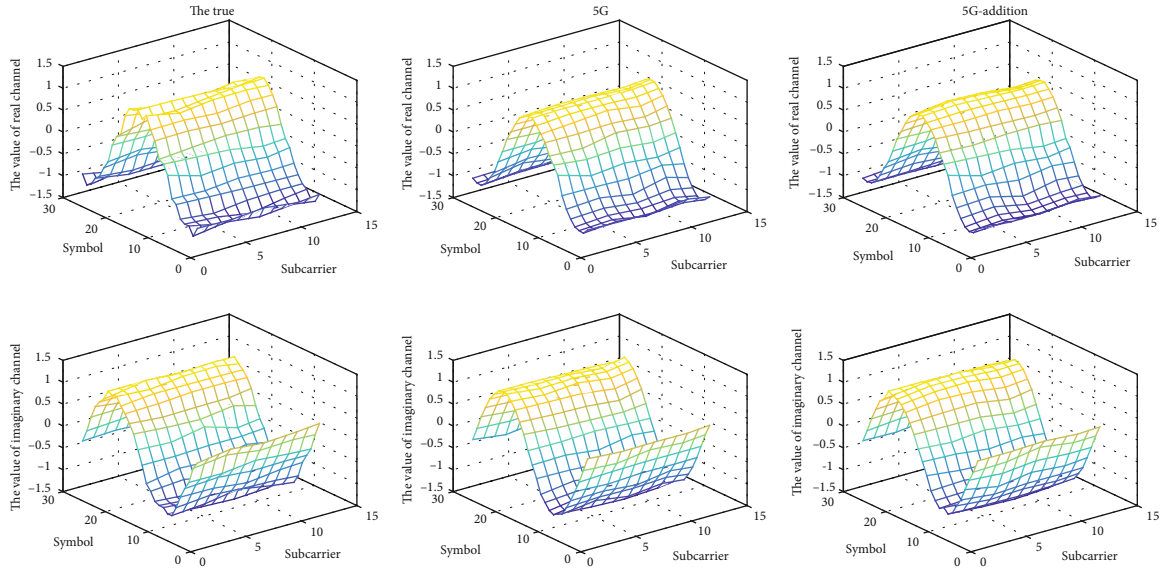

Figure 12: The real part and imaginary part of the channel CSI image predicted by AI-ChannelNet.

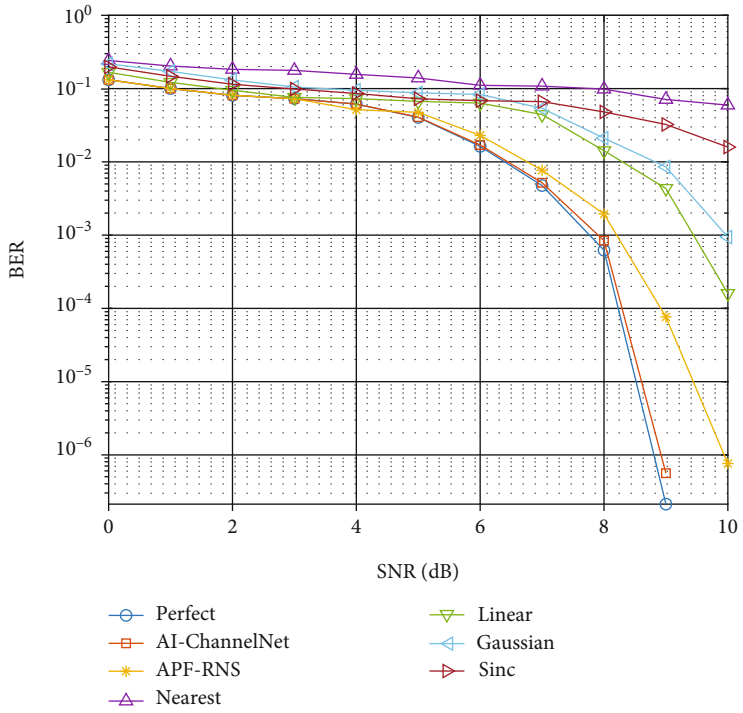

Figure 13: The BER of different methods on the 5G radio frame with $v = 120$ km/h.

As a standard LSTM layer, the FLOP is calculated as follows:

$$\text{FLOP} = 4 \cdot (N_r + D_l + 1) \cdot N_r, \tag{21}$$

where N_r is the number of LSTM neurons and D_l is the constraint length. The size of weight matrices and FLOP are shown in Table 8. The size of the input CSI image is (80, 12, 4); thus, the weight matrix of the LSTM layer is (64 + 80, 12, 4, 64). Besides, the number of LSTM neurons is 64 and the output size is (80, 64). It can be seen that the computation complexity of the proposed algorithm is 811008 FLOP.

Although the computational complexity of the proposed algorithm is obviously larger than that of conventional methods, the performance can be improved significantly through additional complexity. In order to track the channel in time, the neural network was limited

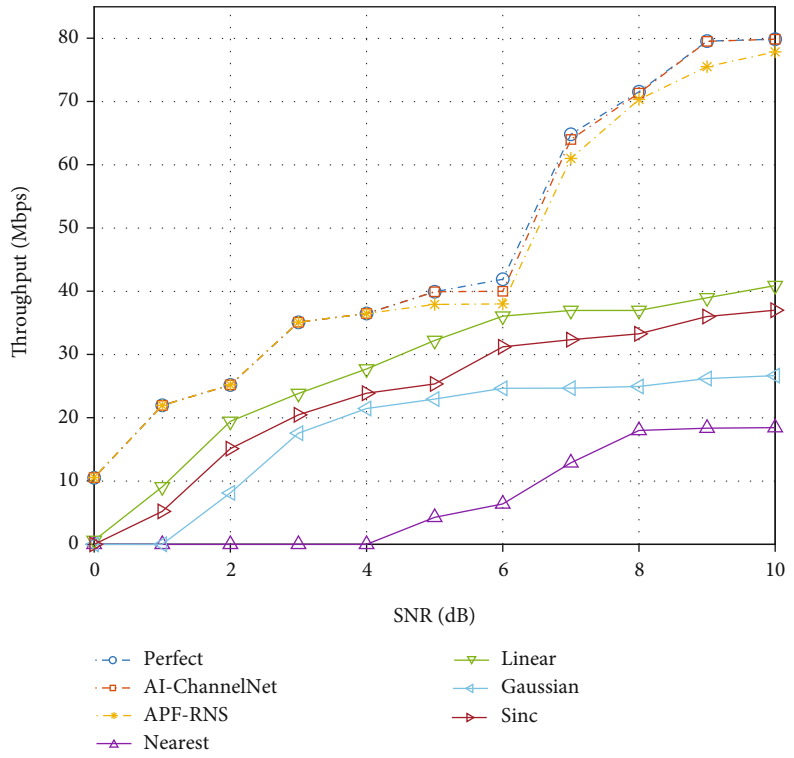

Figure 14: The throughput of different methods on the 5G radio frame with $v = 120$ km/h.

Table 7: The FLOP of AI-ChannelNet (CNN).

Layer	Kernel size	Output size	FLOP
Conv1D	(3, 1, 8)	(80, 1, 16)	3840
Pooling	0	(40, 1, 16)	0
Flatten	0	(640)	0
Dense	(640, 2)	(2)	1280
Summary	—	—	5120

Table 8: The FLOP of AI-ChannelNet (LSTM).

Layer	Kernel size	Output size	FLOP
LSTM	(144, 48, 64)	(80, 64)	442368
Conv1D	(3, 1, 8)	(80, 64, 8)	122880
Pooling	0	(40, 32, 8)	0
Flatten	0	(10240)	0
Softmax	(10240, 24)	(12, 2)	245760
Summary	—	—	811008

to be updated once within 0.5 ms, which is the interval of adjacent RS. Fortunately, the computational ability of CPU/GPU has developed a lot in recent years. For example, the GTX 1080Ti was popular in deep learning research with the 11.3T FLOP, which has sufficient computing power for the proposed algorithm with only 4×10^{-3} ms cost (including training, prediction, and recovery signals). Therefore, the proposed algorithm can be implemented with acceptable computation complexity to track the fast time-varying wireless channel in the high-speed V2I scenario.

5. Conclusion

In this paper, a novel AI-based channel prediction scheme for the 5G wireless system in high-speed V2I scenarios is proposed. In the proposed scheme, the temporal features of the channel in high-speed V2I scenarios are extracted by the integration of CNN and LSTM to present accurate channel information. The predictor is trained in real time based on the historical channel estimation on RS to realize accurate channel prediction and then recovers the received signal according to predicted channel information, which leads to better performance compared to the conventional methods. Through the numerical experiment on the WINNER D2a channel model, more improvement could be achieved by the proposed scheme at a higher speed, e.g., 140 km/h. Besides, the proposed scheme performs well without additional RS in high-speed V2I scenarios, which avoids excessive consumption of transmission resources. The proposed scheme is expected to be applied to the 5G wireless system to improve the communication performance in high-speed V2I scenarios.

Data Availability

The data that support the findings of this study are available from the corresponding author upon reasonable request.

Conflicts of Interest

The authors declare that they have no conflicts of interest.

Acknowledgments

This work was supported by the Key-Area Research and Development Program of Guangdong Province under Grant 2019B010157002, the Fundamental Research Funds for the Central Universities (2020JBZD005), the fund of National Defense Science and Technology Key Laboratory for Equipment Pre Research (No. 6142217200404), the National Natural Science Foundation of China (Grant Nos. U21A20445 and 62001135), and the State Key Laboratory of Rail Traffic Control and Safety under Grant RCS2022ZT013.

References

[1] S. Gyawali, S. Xu, Y. Qian, and R. Q. Hu, "Challenges and solutions for cellular based V2X communications," *In IEEE Communications Surveys and Tutorials*, vol. 23, no. 1, pp. 222–255, 2021.

[2] M. Yang, B. Ai, R. He et al., "V2V channel characterization and modeling for underground parking garages," *In China Communications*, vol. 16, no. 9, pp. 93–105, 2019.

[3] R. Atallah, M. Khabbaz, and C. Assi, "Multihop V2I communications: a feasibility study, modeling, and performance analysis," *In IEEE Transactions on Vehicular Technology*, vol. 66, no. 3, pp. 2801–2810, 2017.

[4] K. Guan, D. He, B. Ai et al., "Millimeter-wave communications for smart rail mobility: from channel modeling to prototyping," in *In IEEE International Conference on Communications Workshops (ICC Workshops)*, pp. 1–6, Shanghai, China, 2019.

[5] B. Ai, A. F. Molisch, M. Rupp, and Z.-D. Zhong, "5G key technologies for smart railways," *Proceedings of the IEEE*, vol. 108, no. 6, pp. 856–893, 2020.

[6] L. He, X. Fang, H. Li, C. Li, and Y. Liu, "An mmWave beamforming scheme for disaster detection in high speed railway," in *In IEEE/CIC International Conference on Communications in China (ICCC)*, pp. 1–6, Chengdu, China, 2016.

[7] X. Chen and P. Fan, "Low-complexity location-aware multiuser massive MIMO beamforming for high speed train communications," in *In IEEE 85th Vehicular Technology Conference (VTC Spring)*, pp. 1–6, Sydney, NSW, Australia, 2017.

[8] Y. Cui and X. Fang, "Performance analysis of massive spatial modulation MIMO in high-speed railway," *IEEE Transactions on Vehicular Technology*, vol. 65, no. 11, pp. 8925–8932, 2016.

[9] H. Jingyu, Z. Xiaomin, X. Zhijiang, and M. Limin, "An adaptive Doppler shift estimator in mobile communication systems," *IEEE Antennas and Wireless Propagation Letters*, vol. 6, pp. 117–121, 2007.

[10] C. Lv, J. Lin, and Z. Yang, "Channel prediction for millimeter wave MIMO-OFDM communications in rapidly time-varying frequency-selective fading channels," *IEEE Access*, vol. 7, pp. 15183–15195, 2019.

[11] Z. Dian Fan, G. W. Zhong, and F. Gao, "Doppler shift estimation for high-speed railway wireless communication systems with large-scale linear antennas," in *In International Workshop on High Mobility Wireless Communications (HMWC)*, pp. 96–100, Xi'an, China, 2015.

[12] B. Ai, C. Briso-Rodriguez, X. Cheng et al., "Challenges toward wireless communications for high-speed railway," *IEEE Transactions on Intelligent Transportation Systems*, vol. 15, no. 5, pp. 2143–2158, 2014.

[13] J. Liao, "Analytical solution of DFT interpolated frequency estimator for Hanning windowed signal," in *In 15th International Symposium on Communications and Information Technologies (ISCIT)*, pp. 177–180, Nara, Japan, 2015.

[14] Y. Liao, S. Sun, X. Shen, S. Zhang, X. Yang, and X. Zhang, "BEM-based channel estimation and interpolation methods for doubly-selective OFDM channel," in *In IEEE International Conference on Smart Internet of Things (SmartIoT)*, pp. 70–75, Xi'an, China, 2018.

[15] J. Baek and J. Seo, "Efficient pilot patterns and channel estimations for MIMO-OFDM systems," *IEEE Transactions on Broadcasting*, vol. 58, no. 4, pp. 648–653, 2012.

[16] G. Wang, Q. Liu, R. He, F. Gao, and C. Tellambura, "Acquisition of channel state information in heterogeneous cloud radio access networks: challenges and research directions," *IEEE Wireless Communications*, vol. 22, no. 3, pp. 100–107, 2015.

[17] M. Yang, B. Ai, R. He, H. Chen, Z. Ma, and Z. Zhong, "Angle-of-arrival estimation for vehicle-to-vehicle communications based on machine learning," in *In International Conference on Wireless Communications and Signal Processing (WCSP)*, pp. 154–158, Nanjing, China, 2020.

[18] W. Lyu, Z. Zhang, C. Jiao, K. Qin, and H. Zhang, "Performance evaluation of channel decoding with deep neural networks," in *In IEEE International Conference on Communications (ICC)*, pp. 1–6, Kansas City, MO, USA, 2018.

[19] Q. Zheng, R. He, B. Ai et al., "Channel non-line-of-sight identification based on convolutional neural networks," *IEEE Wireless Communications Letters*, vol. 9, no. 9, pp. 1500–1504, 2020.

[20] L. Xiong, Z. Zhang, and D. Yao, "A novel real-time channel prediction algorithm in high-speed scenario using convolutional neural network," *Wireless Networks*, vol. 28, no. 2, pp. 621–634, 2022.

[21] C. Luo, J. Ji, Q. Wang, X. Chen, and P. Li, "Channel state information prediction for 5G wireless communications: a deep learning approach," *IEEE Transactions on Network Science and Engineering*, vol. 7, no. 1, pp. 227–236, 2020.

[22] S. H. A. Shah, M. Sharma, and S. Rangan, "LSTM-based multilink prediction for mmWave and sub-THz wireless systems," in *In ICC 2020-2020 IEEE International Conference on Communications (ICC)*, pp. 1–6, Dublin, Ireland, 2020.

[23] Y. Zhu, X. Dong, and T. Lu, "An adaptive and parameter-free recurrent neural structure for wireless channel prediction," *IEEE Transactions on Communications*, vol. 67, no. 11, pp. 8086–8096, 2019.

[24] H. Huang, S. Guo, G. Gui et al., "Deep learning for physical-layer 5G wireless techniques: opportunities, challenges and solutions," *IEEE Wireless Communications*, vol. 27, no. 1, pp. 214–222, 2020.

[25] H. He, S. Jin, C. Wen, F. Gao, G. Y. Li, and Z. Xu, "Model-driven deep learning for physical layer communications," *IEEE Wireless Communications*, vol. 26, no. 5, pp. 77–83, 2019.

[26] R. He, B. Ai, Z. Zhong, A. F. Molisch, R. Chen, and Y. Yang, "A measurement-based stochastic model for high-speed railway channels," *IEEE Transactions on Intelligent Transportation Systems*, vol. 16, no. 3, pp. 1120–1135, 2015.

[27] M. Yusuf, E. Tanghe, F. Challita et al., "Stationarity analysis of V2I radio channel in a suburban environment," *IEEE Transactions on Vehicular Technology*, vol. 68, no. 12, pp. 11532–11542, 2019.

[28] R. He, M. Yang, L. Xiong et al., "Channel measurements and modeling for 5G communication systems at 3.5 GHz band," in *in URSI Asia-Pacific radio science conference (URSI AP-RASC), Seoul*, pp. 1855–1858, Korea (South), 2016.

[29] 3GPP, *NR; Physical Channels and Modulation*, In 3GPP TS 38.211, 2020.

[30] P. Kysti, J. Meinil, L. Hentil, X. Zhao, and T. Rautiainen, *WINNER II Channel Models*, IST-4-027756 WINNER II D1.1.2 V1.2, 2008.

[31] V. Hoang and K. Jo, "Practical analysis on running speed for efficient CNN architecture design," in *In 12th International Conference on Human System Interaction (HSI)*, pp. 221–224, Richmond, VA, USA, 2019.

[32] P. Singh and V. P. Namboodiri, "SkipConv: skip convolution for computationally efficient deep CNNs," in *In 2020 International Joint Conference on Neural Networks (IJCNN)*, pp. 1–8, Glasgow, UK, 2020.